Proceedings of the 20th International Conference on Soil Mechanics and Geotechnical Engineering– Rahman and Jaksa (Eds)

Clay fabric under the brightest light

La structure de l'argile sous la lumière la plus brillante

Georgios Birmpilis & Jelke Dijkstra
Architecture and Civil Engineering, Chalmers University of Technology, Sweden, georgios.birmpilis@chalmers.se

ABSTRACT: For the last six decades synchrotron facilities have utilised high brilliance electromagnetic radiation to reveal the evolving internal structure of a great variety of man-made and natural materials. Lately, an increasing number of such studies is focusing on geomaterials. Thanks to the improved capabilities of synchrotron instruments, for the first time natural sensitive clays can be experimentally studied in their undisturbed, wet state. In this work, the potential of synchrotron-based X-ray methods for monitoring the fabric in a natural clay is demonstrated. The structure of natural clays spans nm - mm. Thus, multiple techniques, covering nano- to micro- scale observations of natural clay samples are combined. X-ray Scattering (XS) and X-ray Computed Tomography (XCT) measurements from two synchrotron facilities (ESRF, France and MaxLab, Sweden) are collected to provide information on the fabric in clays. Quantified measures of fabric evolution, such as interparticle distances and changes in particle orientation are monitored. Images of sub-micron resolution reveal interparticle arrangement of clay and non-clay particles and diffraction data monitor the intraparticle changes as well as providing statistics on fabric orientation.

RÉSUMÉ : Depuis six décennies, au sein des installations de rayonnement synchrotron des rayons électromagnétiques de haute brillance ont été utilisés afin de révéler la structure interne évolutive d'une grande variété des matériaux artificiels ainsi que naturels. Dernièrement, une grande partie de ces études se concentrent sur les géomatériaux. Grâce aux équipements scientifiques de pointe, pour la première fois, des argiles sensibles naturelles peuvent être étudiées de manière expérimentale en leur état humide et non perturbé. Au cours de ce travail, les méthodes prometteuses des rayons X synchrotron pour explorer la structure d'une argile naturelle, sont présentées. La structure des argiles naturelles s'étend sur plusieurs échelles spatiales. Par conséquent, plusieurs techniques qui couvrent les observations nanoscopiques et microscopiques d'échantillons des argiles naturelles sont combinées. Des mesures XS (X-ray Scattering) (XS) et XCT (X-ray Computed Tomography) rendues par les deux installations synchrotron (ESRF, France and MaxLab, Suéde) sont collectées afin de fournir des informations sur la structure. Des mesures quantifiées de l'évolution de la structure, telles que les distances entre les particules et le changement d'orientation des particules, sont enregistrées. Des images de résolution inférieure à l'échelle microscopique révèlent un arrangement entre les particules d'argile et celles de matériaux autres que l'argile et les données de diffraction suivent les changements entre les particules tout en fournissant des données statistiques sur l'orientation de la structure.

KEYWORDS: clay, X-rays, synchrotron, Computed Tomography, scattering

1 INTRODUCTION

High brilliance electromagnetic radiation such as X-rays can be utilised to reveal the evolving internal structure of a great variety of materials. With the capabilities and accessibility of synchrotron facilities improving all the time, these non-invasive radiation methods are increasingly being utilised to study the complex fabric of granular media such as geomaterials. Thus, fine-grained soils can be experimentally studied in their undisturbed state.

1.1 *Synchrotron* facilities

Synchrotrons are particle accelerator facilities that operate as sources of very bright X-ray radiation. This is accomplished by the acceleration of high-energy electrons, by circulation, in a circular system of powerful magnets. One such type of magnets, the bending magnets, is responsible for the deflection of X-rays from their orbit. This deflection is responsible for the emission of X-ray light. The radiation is subsequently corrected on its temporal and spatial coherence, *i.e.* smaller energy bandwidth and angular acceptance of the beam (Weber, 2016). Attributes as high intensity, monochromaticity and spatial focus of the beam produce high brilliance (the measure of the desired qualities for quantitative imaging). Synchrotron facilities produce typically 10^{13} times more brilliant X-rays compared to laboratory X-ray sources. This means that the temporal resolution can reach femtoseconds time and spatial resolution approached sub-micron levels.

1.2 *X-ray Imaging and Scattering*

Due to their high energy, X-rays intrude matter and interact with it in different manners: photoelectric absorption, inelastic and elastic scattering, pair production of electrons and photodisintegration (Cartz, 1995). Nevertheless, two phenomena are mostly used to study quantitatively the elemental composition of materials: the disruption or the change of the X-ray trajectory. Two basic respective methodologies are developed with the use of X-rays: imaging, mainly based on the absorption and refraction of the radiation, and scattering, which utilises the angle of deviation of X-rays from their initial trajectory.

Absorption-based imaging is a well-established imaging technique developed over the last century, that is familiar to most by medical radiography. Radiography is the product of transmitted X–ray radiation captured by an X-ray sensitive detector or film. Transmission is the contrasted result of absorption of X-rays after their reaction with the electrons of atoms in matter. Therefore, high absorption (or lower transmission) is linked with a larger number of atoms. This signifies either the presence of a larger number of atoms in the illuminated volume, *i.e.* a measure of relative density, or the presence of atoms with high atomic number, *i.e.* phase identification. This concept of electron density mapping in a sample, finds an unparalleled match with engineering applications in the field of material science. Nevertheless, radiography provides a 2D mapping of the attenuation paths through the sample and cannot resolve attenuation differences along the path (depth). A great imaging development was the

computing of the 3D image attenuation field from radiographies at incremental projection angles through reconstruction algorithms (Feldkamp et al., 1984). X-ray Computed Tomography (XCT) has been a valuable medical imaging tool already since the 1970s. Since then, XCT has been combined with Digital Volume Correlation (DVC) for the quantification of deformations in solids and fluids as well as the evolving flow patterns (Sutton et al., 2009; Adrian et al., 2011). The principle of DVC is based on the mathematical comparison of a pair of digital images acquired at different instances of the experiment and relies on the contrast of the two images that can be correlated. On the contrary, elastic X-ray scattering occurs when X-ray radiation excites electrons to oscillate in the same frequency. The interference of an incident X-ray with a crystal structure of characteristic d spacing is constructive when Bragg's law is satisfied:

$$n\lambda = 2dsin\theta \quad (1)$$

X-ray Scattering (XS) is a family of non-destructive methods which provides bulk measurements of the structure of scatterers in the nm to μm range. Small Angle X-ray Scattering (SAXS) refers to very low scattering angles (0.1°-10°) that can allow capturing of heterogeneities in the submicron range. For even larger colloidal spacing, Ultra Small Angle X-ray Scattering (USAXS) an extension of SAXS can be used. Wide Angle X-ray Scattering (WAXS) is positioned in between SAXS and diffraction for high scattering angles that resolve the internal structures of crystals.

1.3 *Geomaterials in Synchrotrons*

The properties of synchrotron radiation described above indicate that these type of methods are ideal for the study of the internal structures of geomaterials. Soils and rocks are typically comprised by the grains of varying density and mineralogy. Thus, the use of imaging, scattering or the combination of both are ideal for observation of internal structures of geomaterials.

Arthur (1962) and Roscoe et al. (1963) were the first to employ X-ray imaging to obtain observation of internal soil fabric. Since then great advances have been made for testing coarse grained geo-materials with simultaneous monitoring of the internal mechanisms using XCT mainly in laboratory X-ray sources (Desrues et al., 1996; Alshibli and Hasan, 2008; Hall et al., 2010; Andò et al., 2012). Additionally, *in-operando* XCT imaging combined with DVC analysis (*e.g.* Stamati et al., 2020), can provide a detailed description of the kinematics at particle level for coarse-grained soils. The superiority, however, of synchrotron radiation have started to attract interest for the study of soil behaviour with the highest available spatial and temporal resolution (Matsushima et al., 2010; Hall and Wright, 2015; Andò et al., 2019). Lenoir et al. (2007) utilized X-ray imaging to capture the deformation and failure mechanics in fine-grained argillaceous rocks.

X-ray diffraction was established early as the principal method for the identification of mineral composition of soils and rocks (Grim 1953). X-rays are ideal for the study of structures at nanometre scale due to their wavelength range (10 pm – 10 nm). The method can provide diverse information about the composition, particle morphology as well as the particle distribution particulate systems. Nevertheless, due to the complexity and the high particle density of natural fine-grained soils XS has until now mainly been used for research on clay suspensions (Morvan, 1994; Pignon, 1997; Saunders, 1999; Zhang, 2003; Pujari, 2011).

The present paper summarises an experimental campaign in different synchrotron imaging and scattering facilities in order to study the internal multiscale fabric of natural sensitive soft clay from Western Sweden.

2 METHODOLOGY

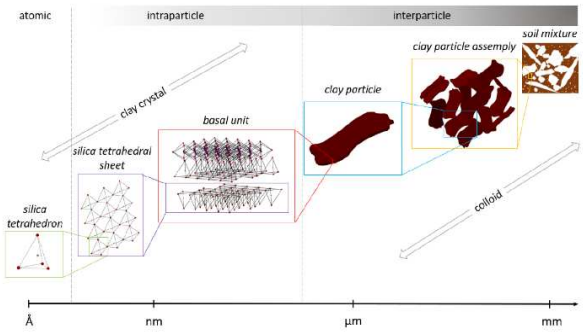

Figure 1. Schematic of the hierarchical structure of clay (Birmpilis, 2020).

Fine-grained sensitive soils typically comprise of mixtures of clay and silt particles at high water contents. The resulting fabric spans from nano- to millimetre scale in hierarchical structures as schematically presented in Figure 1. In order to navigate through the different scales of fabric a scheme that combines both scattering and imaging techniques is designed.

2.1 *Material*

The study case material in this work is a natural sensitive clay of medium sensitivity and large silt content from 6 m depth from the well-characterised Utby test site (Figure 2) in Gothenburg, Sweden (Karlsson et al., 2016; Li et al., 2018; Birmpilis et al., 2019). The natural water content (w_N) at the layer was 80% and the sensitivity value (S_t) was below 30, bulk density (ρ) at 1.6 g/cm^3, clay content larger than 50% and liquid limit (w_L) of 55%.

Figure 2. The Utby test site is located in the outskirts of Gothenburg city, in the Western coast of Sweden.

2.2 *Sample miniaturisation*

A basic requirement of synchrotron radiation techniques is the miniaturisation of the sample to satisfy sufficient transmission of X-rays through the sample and thus a high signal-to-noise ratio. This limits the sample thickness to the micro- to milli- metre range. X-ray translucent borosilicate capillaries were used to host the soil samples preserving their natural water content and the intact structure when the sample thickness was reduced to smaller than 10 mm (Birmpilis et al., 2019). Figure 3 demonstrates the specimen environment in two different beamlines, MaxLab I991-4 in Lund Sweden, and ESRF-ID16 Grenoble, France. Rectangular capillary tubes, 6.50 mm x 1.40 mm outer dimensions, 0.16 mm wall thickness, were used at the I911-4 SAXS instrument (Figure 3), with a sample height of 30 mm. SAXS measurements were complemented with surface Digital Image Correlation (DIC) using a two camera stereoscopic system. Thus, the change in intraparticle scale could be linked to the simultaneous total height reduction. For the needs of

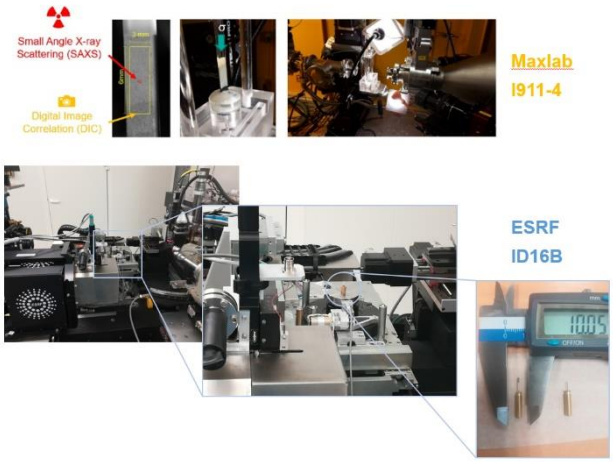

Figure 3: Different miniaturised specimens and testing set ups were designed to be compatible with the beamline environment.

nanotomography in ID16B, micrometre scale sampling was required, so glass capillaries with 300μm diameter and 10 μm wall thickness were used. Finally, the XCLAY triaxial cell (Birmpilis, 2020) was used to facilitate 20mm height, 10 mm diameter samples at ID19.

2.3 *Facilities*

The experimental campaign includes beamtimes in three different beamlines for scattering and imaging: I911-4 SAXS beamline in Maxlab, Lund, Sweden (Labrador et al., 2013); ID16B nanotomography beamline in the European Synchrotron Radiation Facility (ESRF), Grenoble, France (Weitkamp et al., 2010; Boller, 2017); and ID19 microtomography beamline in ESRF.

3 RESULTS

In this section, results of X-ray based non-invasive techniques are presented to concatenate information regarding fabric spacing and particle orientation from intra- and inter- particle scale.

Starting from the nanoscale and intraparticle observation SAXS is capable to provide information from the crystal structure and specification the basal units types contained in the soil, thus identifying the mineralogy of the mixture. Utby clay consists of two basic minerals, illite and montmorillonite, as identified by the respective peaks in the q – photon intensity graph (Figure 4).

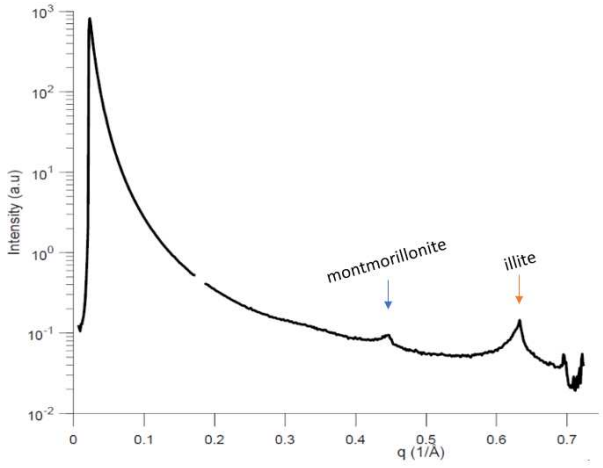

Figure 4: The two clay minerals are identified as peaks in the photon intensity curve of SAXS signal.

The great advantage of non-invasive techniques as SAXS compared to traditional powder diffraction is that the observation of d-spacing can be continuous during hydro-mechanical probing. Additionally, the monitoring of d-spacing distribution around the azimuth can indirectly provide insight on the independent evolution of principal orientation for particles of different mineralogy. The measurements are results of the interaction of X-rays with thousands of clay particles through the illuminated volume, thus act as bulk measurement of the particle response. Figure 5 presents the evolution of principal orientation for the two minerals contained in Utby clay during different stages of compression. The angle of principal orientation is the

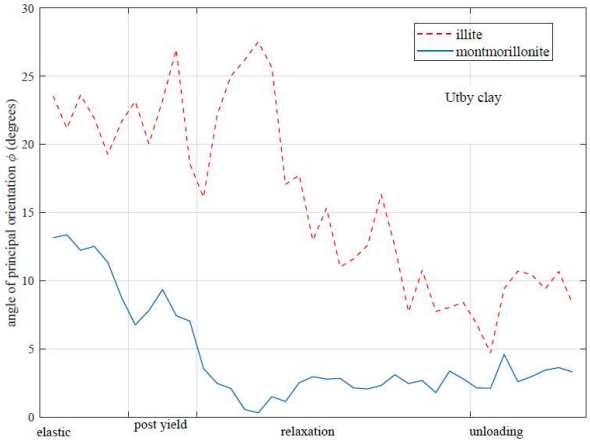

Figure 5: Orientation evolution of the clay fabric during one-dimensional compression (data from Birmpilis et al., 2019).

angle off the horizontal for the majority of the scatterers. A notable aspect of the orientation changes is that while the trend of average rotation towards the horizontal direction is common for the two minerals, they differ in absolute orientation values. This observation raises interest on the actual geometrical arrangement of the particles in space.

High resolution 3D imaging can resolve spatial features and inform qualitatively and quantitatively on particle geometrical arrangements. For the case of fine-grained soils, the resolution requirements are even higher, due to the small particle size and the low contrast between water and clay. Therefore, two high resolution beamlines were employed for this purpose, ID16B and ID19 in ESRF. The acquired images had a wide range of magnifications and resulting resolutions. The voxel sizes spanned from 25nm (nanotomography) to 0.3 μm; 1.3 μm and 6.5 μm (microtomography). The nanotomography data offer

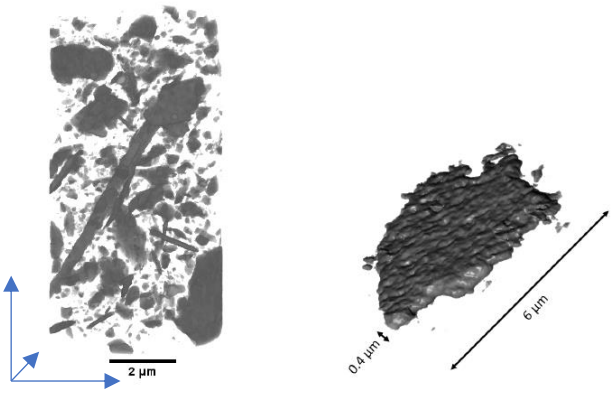

Figure 6: 3D reconstruction of the segmented structure of the near-μm particles (rock flour) on the left and an isolated particle on the right.

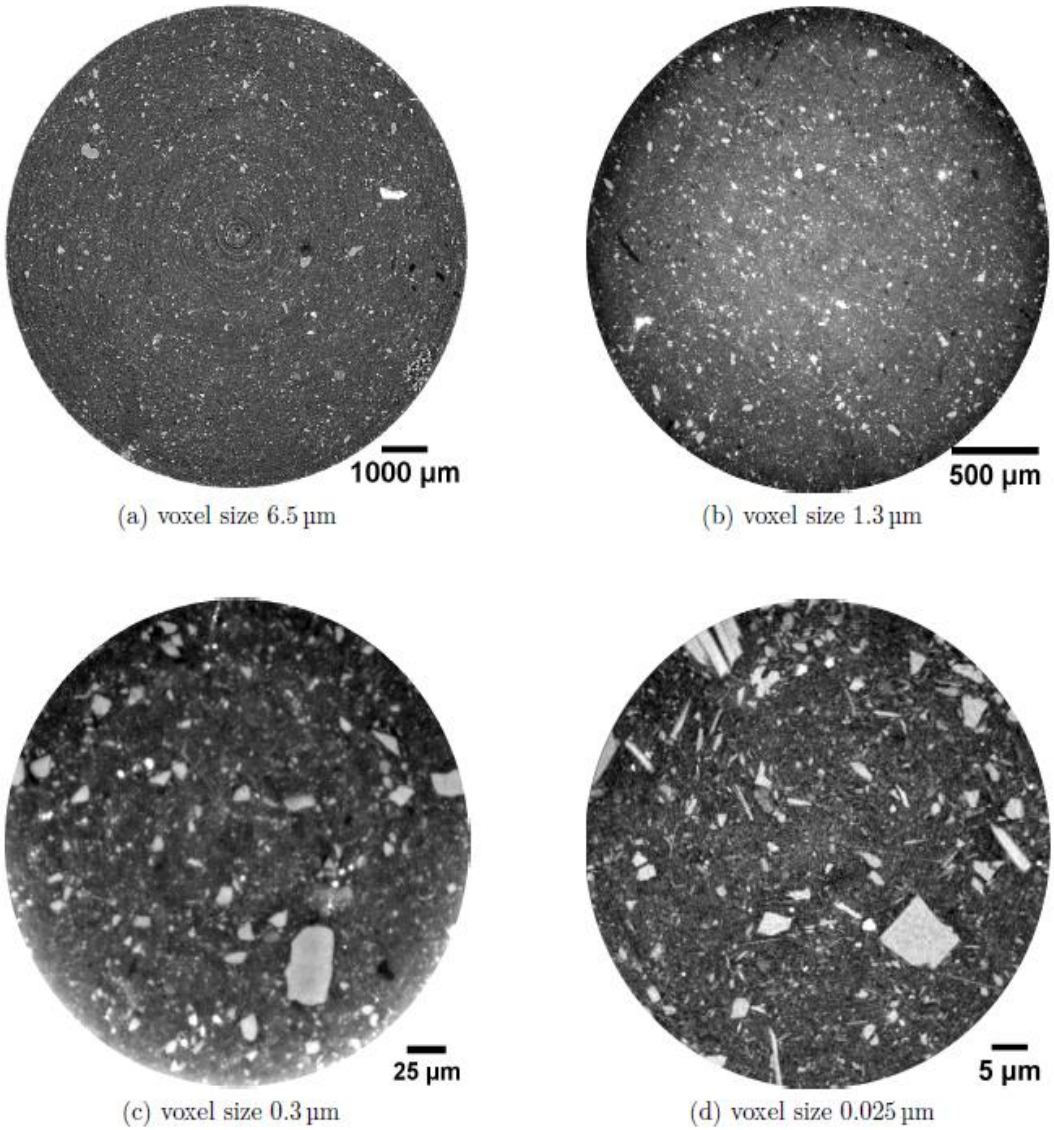

(a) voxel size 6.5 µm (b) voxel size 1.3 µm

(c) voxel size 0.3 µm (d) voxel size 0.025 µm

Figure 7: Tomographies of sensitive clay samples from Utby at different magnification levels from ID19 (a-c) and ID16 (d).

unpresented resolution for imaging of natural clay in its natural, intact state. This was achieved due to phase contrast, which is based on the heterogeneity of refractive index between features in the sample and produces edge enhancement of features such as clay particles, improving uniquely the tomographic quality. The three-dimensional particle arrangement of flaky clay particles is presented in a reconstruction of the segmented image for the near-μm particles (Figure 6; left). An isolated particle is presented on the right part of Figure 6. The aspect ratio of the particles presented in Figure 6 ranges from 1 to 16.

Additionally to the nanotomography, consecutive microtomographies in multiple magnification ratios can demonstrate the repetition of the pattern of silt grain dispersion in the clay matrix at different scales, from millimeter to micrometer. Cross sections of each tomographic image are presented in Figure 7. In Figure 7d, the nanotomography reveals that a big fraction of clay matrix is gauged in sizes substantially smaller than 1 μm. This could potentially be linked to the different response of the two minerals as observed by SAXS, explaining why the two minerals exhibit distinct absolute principal orientation. Such a unique dataset of 3D volumes contains a great number of particles and can be used for statistical interpretation equivalent to the averaging performed physically by scattering.

4 CONCLUSIONS

The present work demonstrates a collection of results on measurements of the multiscale fabric of natural sensitive soft Utby clay from Western Sweden. Synchrotron X-ray based techniques are combined to span observations of fabric, *i.e.* spacing and orientation, from nano- to milli- metre scale. At nanoscale (between 0.7 nm to 20 nm), the intraparticle characteristic d-spacing of the clay minerals (appearing as the respective peaks in the intensity graphs) is monitored, as well as the orientational evolution of the particles is traced for the two identified mineral types (illite and montmorillonite). The two minerals present similar trends of orientation evolution, approaching to the horizontal direction during the one-dimensional compression in the miniature capillary cell, but dissimilar absolute orientation.

The nano-scale scattering data was complemented with a unique 3D image dataset on an intact, wet sample of sensitive clay. The high spatial resolution with voxel size of 25 nm (real resolution approximated at 200 nm) captures, for the first time, the internal 3D structure within the clay sample in its natural

water content. The repeating presence of non-active particles, such as silt, in the mesoscale fabric is observed, down to sub-µm scale. Elongated particles larger than 2 µm and nano-grains form the finer fractions in the sensitive clay were also discerned. The finer clay fraction (<500 nm) could not be distinguished, however, even at this resolution, indicating that this sensitive clay has a large fraction of nanoparticles. The nanometer voxel size provided in this work approached the limit of the achievable resolution for contemporary X-ray tomography.

The aim of this work was to utilise state-of-the-art technology and facilities developed for the most modern material science research. It is demonstrated that soft soil mechanics can be extended outside of the limits of the geotechnical laboratory in order to collect new knowledge on the fundamentals that underpin behaviour of fine-grained soils. For this purpose, necessary adaptations such as sample miniaturisation, design of bespoke testing devices and updated experimental routines must be developed.

5 ACKNOWLEDGEMENTS

The financial support of Vetenskapsrådet, and Swedish Transport Administration (Trafikverket) is greatly appreciated. Maxlab, Sweden, and the European Synchrotron Radiation Facility (ESRF), France, are greatly acknowledged for the granted beamtime and the support provided by their personnel. The help of Ilias Papafotiou is highly appreciated for his adaptation of the abstract in French.

6 REFERENCES

Adrian, L., R.J. Adrian, and J. Westerweel (2011). *Particle image velocimetry*. Cambridge, UK: Cambridge university press.

Alshibli K., and Hasan A. 2008. Spatial variation of void ratio and shear band thickness in sand using X-ray computed tomography. Géotechnique, 58 (4), 249–257.

Andó E., Viggiani S. H. G., Desrues D., and Bésuelle P. 2012. Grain-scale experimental investigation of localised deformation in sand: a discrete particle tracking approach. *Acta Geotechnica*, 7 (1), 1–13.

Andó E., Dijkstra J., Roubin E., Dano C and Boller E. 2019. A peek into the origin of creep in sand. *Granular Matter*, 21 (11) http://dx.doi.org/10.1007/s10035-018-0863-5

Arthur, J., 1962. Strains and lateral force in sands. Ph.D. thesis, University of Cambridge.

Birmpilis, G., Hall S.A., Lages S. and Dijkstra J. 2019. Monitoring of the nano-structure response of natural clay under mechanical perturbation using Small Angle X-ray Scattering and Digital Image Correlation. Acta Geotechnica, 14 (6), 1965–1975, doi:doi.org/10.1007/s11440-019-00832-8.

Birmpilis G. 2020. *Multi-scale fabric evolution during hydro-mechanical probing of fine-grained soils*. PhD Thesis. Chalmers University of Technology, Gothenburg, Sweden.

Boller E., Tafforeau P., Rack A., Fernandez V., Helfen L., Rénier M., Valade J., Vitoux H., Villanova J., Cloetens P, et al. 2017. Synchrotron-tomography with micro, nano and high temporal resolution for industrial and academic use. *Proceedings ICTMS*

Cartz L. 1995. Nondestructive Testing. *Ohio: ASM International*

Desrues, J., Chambon R., Mokni M., and Mazerollet F.. 1996. Void ratio evolution inside shear bands in triaxial sand specimens studied by computed tomography. *Géotechnique*, 46 (3), 529–546

Feldkamp L.A., Davis L.C., and Kress J.W. 1984. Practical cone-beam algorithm. *Journal of the Optical Society of America A* 1, 6, 612–619

Grim, R.E. 1953. *Clay Mineralogy*. New York: McGraw-Hill Book Company, Inc.

Hall S. A., Bornert M., Desrues J., Pannier Y., Lenoir N., Viggiani G., and Bésuelle P. 2010. Discrete and continuum analysis of localised deformation in sand using X-ray CT and volumetric digital image correlation. *Géotechnique*, 60 (5), 315–322.

Hall S.A., Wright J. 2015. Three-dimensional experimental granular mechanics. *Géotechnique Letters,* 5 (4), 236-242.

Karlsson M., Emdal A., and Dijkstra J. 2016. Consequences of sample disturbance when predicting long-term settlements in soft clay. *Canadian Geotechnical Journal*, 1–13, doi:10.1139/cgj-2016-0129.

Labrador A, Cerenius Y, Svensson C, Theodor K, Plivelic T 2013. The yellow mini-hutch for SAXS experiments at MAX IV Laboratory. *J Phys Conf Ser* 425:072019

Lee S., Fischer T.B., Stokes M.R., Klingler R.J., Ilavsky J., McCarty D.K., Wigand M.O., Derkowski A. and Winans R.E. 2014. Dehydration Effect on the Pore Size, Porosity, and Fractal Parameters of Shale Rocks: Ultrasmall-Angle X-ray Scattering Study. *Energy Fuels*, 28 (11), 6772–6779.

Lenoir N., Bornert M., Desrues J., Bésuelle P., and Viggiani G. 2007. Volumetric digital image correlation applied to X-ray microtomography images from triaxial compression tests on argillaceous rock. *Strain*, 43, 193–205.

Leu L., Georgiadis A., Blunt M.J., Busch A., Bertier P., Schweinar K, Liebi M., Menzel A. and Ott H. 2016. Multiscale Description of Shale Pore Systems by Scanning SAXS and WAXS Microscopy. *Energy Fuels*, 30 (12), 1028210297.

Li Y., Dijkstra J., and Karstunen M. 2018. Thermomechanical creep in sensitive clays. *Journal of Geotechnical and Geoenvironmental Engineering*, 144 (11), article 04018 085.

Martínez-Criado G., Villanova J., Tucoulou R., Salomon D., Suuronen J.-P., Labouré S., Guilloud C., Valls V., Barrett R., Gagliardini E., Dabin Y., Baker R., Bohic S., Cohen C., and Morse J. 2016. ID16B: a hard X-ray nanoprobe beamline at the ESRF for nano-analysis. *Journal of Synchrotron Radiation*, 23 (1), 344–352. doi: 10.1107/S1600577515019839.

Matsushima T., Uesugi K., Nakano T., and Tsuchiyama A. 2010. Visualization of grain motion inside a triaxial specimen by micro X-ray CT at SPring-8, *Advances in X-ray Tomography for Geomaterials*, John Wiley & Sons, Ltd, 255–261.

Morvan M., Espinat D., Lambard J. & Zemb Th. 1994. Ultra small and small angle X-ray scattering of smectite clay suspensions. *Colloids and Surfaces A: Physicochemical and Engineering Aspects* 82 (2), 193–203.

Pignon F., Magnin A., Piau J-M., Cabane B., Lindner P. and Diat O. 1997. Yield stress thixotropic clay suspension: Investigations of structure by light, neutron, and X-ray scattering. *Phys. Rev. E,* 56 (3), 3281–3289.

Pujari A., Dougherty L., Mobuchon C., Carreau P.J., Heuzey M.C. and Burghardt W.R. 2011. X-ray scattering measurements of particle orientation in a sheared polymer/clay dispersion. *Rheologica Acta* 50 (1), 3–16.

Roscoe, K., Arthur J., and James R. 1963: The determination of strains in soils by an X-ray method. *Civ. Eng. Public Works Rev.*, 85, 873–876 and 1009–1012.

Saunders J.M., Goodwin J.W., Richardson R.M., and Vincent B. 1999. A Small-Angle X-ray Scattering Study of the Structure of Aqueous Laponite Dispersions. *The Journal of Physical Chemistry B*, 103 (43), 9211-9218, DOI: 10.1021/jp9907185.

Stamati, O., Andó E., Roubin E., Cailletaud R., Wiebicke M., Pinzon G., Couture C., Hurley R.C., Caulk R., Caillerie D., Matsushima T., Bésuelle P., Bertoni F., Arnaud T., Ortega Laborin A., Rorato R., Sun Y., Tengattini A., Okubadejo O., Colliat J.-B., Saadatfar M., Garcia F.E., Papazoglou C., Vego I., Brisard S., Dijkstra J. and Birmpilis G. 2020. spam: Software for Practical Analysis of Materials. The Journal of Open Source Software, 5(51), 2286.

Sutton M.A., Orteu J.J., and Schreier H. 2009. *Image correlation for shape, motion and deformation measurements: basic concepts, theory and applications*. Springer Science & Business Media.

Weber, L. 2016. *Iterative tomographic X-Ray phase reconstruction*. PhD thesis. L'Institut National des Sciences Appliquées de Lyon.

Weitkamp T., Tafforeau P., Boller E., Cloetens P., Valade J.-P., Bernard P., Peyrin F., Ludwig W., Helfen L., Baruchel J. 2010. Status and evolution of the ESRF beamline ID19. *AIP Conference Proceedings*, 1221 (1), 33–38.

Zhang L., Jahns C., Hsiao B. S. and Chu B. 2003. Synchrotron SAXS/WAXD and rheological studies of clay suspensions in silicone fluid. *Journal of Colloid and Interface Science*, 266 (2), 339-345.